

β -Tubulin Isotypes Purified from Bovine Brain Have Different Relative Stabilities[†]

Patricia M. Schwarz, John R. Liggins,[‡] and Richard F. Ludueña*

Department of Biochemistry, The University of Texas Health Science Center at San Antonio, 7703 Floyd Curl Drive, San Antonio, Texas 78284-7760

Received November 10, 1997; Revised Manuscript Received January 26, 1998

ABSTRACT: The highly conserved nature and tissue specificity of the seven vertebrate β -tubulin isotypes provide circumstantial evidence that functional differences among isotypes may exist in vivo. Compelling evidence from studies of bovine brain β -isotypes indicated significant conformational and functional differences in vitro and implied that these differences could be related to in vivo function. A previously uninvestigated parameter of potential importance in assessing functional significance is molecular stability. We examined the relative stability of $\alpha\beta_{II}$ and $\alpha\beta_{III}$ tubulin dimers purified from bovine brain. The use of probes to monitor the exposure of hydrophobic areas and sulfhydryls and the loss of colchicine binding, all of which are known to accompany tubulin's time-dependent loss of function, showed an acceleration of these criteria in $\alpha\beta_{II}$ relative to $\alpha\beta_{III}$ when the isotypes were incubated at 37 °C. Studies using differential scanning calorimetry suggested that unfolding of the isotypes at ~60 °C and decay at 0 °C were both highly cooperative. It was also observed that $\alpha\beta_{III}$ had a higher melting temperature and a larger population of molecules retaining tertiary structure after incubation at 0 °C for 20 h. These studies support the conclusion that $\alpha\beta_{III}$ is significantly more stable than $\alpha\beta_{II}$ and raise the possibility that differences in relative stabilities of tubulin isotypes may be important in regulating the functional properties of microtubules in vivo.

Tubulin, the major component of microtubules, is an $\alpha\beta$ heterodimer. The complexity of this ubiquitous protein is due in part to the fact that both subunits exist as several isotypic forms which differ in their amino acid sequences. The β -isotype family in vertebrates is very highly conserved. Homologous β -isotypes from two different species often have greater homology to one another than either isotype has to the other β -isotypes of the same species (1). This high degree of conservatism is consistent with the hypothesis that the β -isotypes have functional significance. The fact that the β -isotypes have tissue-specific distributions is also consistent with this hypothesis. Of the seven β -isotypes found in vertebrates, β_I and β_{IVb} are constitutive, β_{II} and β_{IVa} are found largely in the brain and nervous system, β_{III} is restricted to neurons and a small number of other cell types, and β_{VI} is found in hematopoietic tissue, while the distribution of β_V is unknown (1). Monoclonal antibodies to the β_{II} , β_{III} , and β_{IV} subunits of bovine brain tubulin have been used to purify tubulin which is homogeneous with respect to the β -subunit (2). The isotypically purified dimers have been shown to assemble at different rates (2) into microtubules with different dynamic properties (3) and to differ in their ligand-binding properties as well as their conformations (4–7). In general, by most of the assays used, $\alpha\beta_{II}$ and $\alpha\beta_{IV}$

differ only slightly from each other, but differ greatly from $\alpha\beta_{III}$; this is consistent with their sequences.

It is not currently known whether the in vitro differences being revealed by these studies are representative of differences in vivo. While some studies indicate that β -isotypes are functionally interchangeable and show the cytoskeletal microtubules to be indiscriminately composed of all available isotypes (8), other studies have shown unique cellular distributions (9) and evidence of in vivo differences in stability (10) and function (11) among β -isotypes. In neurons, there is evidence to indicate that microtubules with different biochemical properties coexist (12), and from studies using cultured animal cells, there is evidence that cells can distinguish between and regulate the levels of individual isotypes (13). It has been suggested that the existence of the β -isotype family may provide cells with a means of regulating the dynamic behavior of their microtubules by adjusting the relative amounts of the isotypes (1).

In addition to ligand-binding and dynamic properties, a parameter of potential importance in assessing the functional significance of tubulin isotypes is the stability of the molecule. This is particularly important in the case of tubulin which has long been known to be an unstable molecule and to lose its functional properties in vitro in a time-dependent process known as decay. Tubulin loses the ability to bind drugs such as colchicine (14); in addition, sulfhydryl groups (15) and hydrophobic areas (16) become exposed.

The relative stability of tubulin isotypes in vitro has not hitherto been examined. Accordingly, we have purified tubulin dimers isotypically homogeneous for their β -subunit

[†] This research was supported by Grants CA 26376 from the National Institutes of Health and AQ-0726 from the Robert A. Welch Foundation to R.F.L. This research was supported in part by a Cancer Center Support Grant from the National Cancer Institute, P30 CA 54174.

* Corresponding author. Phone: 210-567-3732. Fax: 210-567-6595.

[‡] Present address: Department of Biology, The Johns Hopkins University, 3400 North Charles Street, Baltimore, MD 21218.

and have compared their stability using a variety of probes. We have examined the exposure of hydrophobic areas and sulfhydryl groups and the loss of colchicine binding. We have also used differential scanning microcalorimetry to measure the changes in tertiary structure associated with decay. By all criteria, $\alpha\beta_{III}$ was found to be significantly more stable than $\alpha\beta_{II}$. These results raise the possibility that relative differences in stability among tubulin isotypes may be an important part of the regulation of the properties of cellular microtubules.

EXPERIMENTAL PROCEDURES

Preparation of β -Tubulin Isotypes. Microtubule protein was purified from bovine cerebra and chromatographed on phosphocellulose to obtain pure tubulin (17). Tubulin was further purified by immunoaffinity chromatography to obtain the isotypically purified $\alpha\beta_{II}$ and $\alpha\beta_{III}$ dimers (2).

Fluorescence Measurements. Samples of $\alpha\beta_{II}$ and $\alpha\beta_{III}$ were incubated in 0.1 M MES,¹ pH 6.4, 1 mM EGTA, 0.1 mM EDTA, 0.5 mM $MgCl_2$, and 1 mM GTP (MES buffer) at 37 °C. At various time intervals, aliquots of each dimer were incubated with the fluorescent apolar probe bis(1,8-anilinonaphthalenesulfonate) (BisANS) to detect hydrophobic areas that became exposed to the solvent during decay (16). Measurements were made in a Hitachi F-2000 fluorescence spectrophotometer. Samples were excited at 385 nm and the emission was measured at 490 nm. Corrections for inner filter effect were made when comparing samples containing different BisANS concentrations using the formula

$$F_{cor} = F_{obs} \times \text{antilog}[(A_{ex} + A_{em})/2]$$

where A_{ex} and A_{em} are the absorbance values at the excitation and emission wavelengths, respectively.

Alkylation of Tubulin. Samples of $\alpha\beta_{II}$ and $\alpha\beta_{III}$ were incubated in MES buffer at 37 °C to induce decay. At various time intervals, aliquots of each dimer were reacted with iodo[¹⁴C]acetamide for 1 h at 37 °C to monitor the exposure of sulfhydryls. Incorporation of the label was measured by precipitating the tubulin with trichloroacetic acid, filtering the precipitated samples, and determining the radioactivity of the filters (18).

Colchicine Binding. To assess the stability of the colchicine-binding site, samples of $\alpha\beta_{II}$ and $\alpha\beta_{III}$ were incubated in MES buffer at 37 °C. At various times during the incubation, aliquots of $\alpha\beta_{II}$ and $\alpha\beta_{III}$ were reacted with [³H]-colchicine for 2 h at 37 °C. The binding of [³H]colchicine to tubulin was determined by filtration using DEAE-cellulose filters (19).

Differential Scanning Microcalorimetry. Scanning microcalorimetry was performed in an MC-2 microcalorimeter from MicroCal, Inc. Samples of $\alpha\beta_{II}$ and $\alpha\beta_{III}$ were incubated in 0.05 M PIPES, pH 7.0, 1 mM EGTA, 0.5 mM $MgCl_2$, and 1 mM GTP at 0 °C (PIPES buffer). At various time intervals, aliquots of the isotypically purified dimers were subjected to upward scans from 10 °C to at least 75

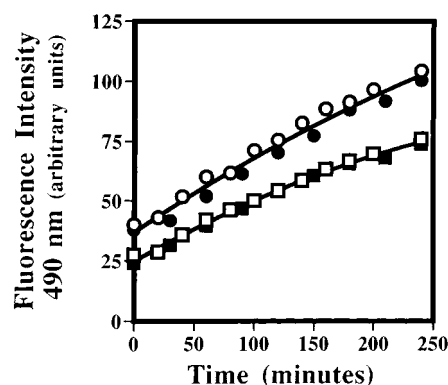


FIGURE 1: Exposure of hydrophobic areas on $\alpha\beta_{II}$ and $\alpha\beta_{III}$ during decay. Data presented are from two identical experiments. Samples of $\alpha\beta_{II}$ [data sets one (○) and two (●)] and $\alpha\beta_{III}$ [data sets one (□) and two (■)] at 2 μ M were incubated at 37 °C for 4 h. At various time intervals, aliquots were removed and made 10 μ M in BisANS. The fluorescence intensity was measured immediately.

°C and sometimes 100 °C. The scanning rate was 70 °C h^{-1} . Data were analyzed using an Origin computer program supplied by MicroCal, Inc. (20). Calorimetry scans of tubulin were also performed in the same MES buffer as the other decay experiments. The profiles of the leading edge of the unfolding transition and the melting temperature were identical. In MES buffer, however, aggregation often occurred a few degrees above the melting temperature, resulting in an exothermic peak which obscured the trailing edge of the unfolding transition, precluding quantitative analysis of the heat capacity of the tubulin samples. Hence, further calorimetry experiments were performed in PIPES buffer.

RESULTS

The fluorescent probe BisANS was used to monitor the appearance of hydrophobic areas of the $\alpha\beta_{II}$ and $\alpha\beta_{III}$ dimers over time. Figure 1 shows the patterns obtained when the isotypically purified dimers were incubated for 4 h in the absence of BisANS at 37 °C. The concentrations of the dimers were 2 μ M; BisANS was added to a final concentration of 10 μ M just prior to measuring the fluorescence intensity. The graph is a composite of data points collected in two separate experiments and shows that the rate of increase of fluorescence intensity was faster for BisANS binding to $\alpha\beta_{II}$ than to $\alpha\beta_{III}$. For example, in $\alpha\beta_{II}$, over a period of 4 h, the BisANS-induced fluorescence increased by 63 ± 1 units, while in $\alpha\beta_{III}$, over the same period, the BisANS-induced fluorescence increased by only 49 ± 1 units. Clearly, the rate of increase in BisANS binding decreased during the experiment; however, over any given time period within the experiment, BisANS binding by $\alpha\beta_{II}$ always increased more than did BisANS binding by $\alpha\beta_{III}$. It was also observed that $\alpha\beta_{II}$ initially bound more BisANS than did $\alpha\beta_{III}$. The concentration-dependent binding of BisANS to $\alpha\beta_{II}$ and $\alpha\beta_{III}$ is shown in Figure 2. Here, BisANS concentrations ranged from 0.2 to 10 μ M. BisANS was mixed with the isotype samples immediately before the fluorescence intensity was measured. At BisANS:tubulin ratios of less than 1:1, binding of the probe to both isotypes was comparable. At stoichiometric ratios greater than 1:1, the fluorescence intensity of BisANS bound to $\alpha\beta_{II}$ was higher than that of BisANS bound to $\alpha\beta_{III}$. At 10 μ M

¹ Abbreviations: BisANS, bis(1,8-anilinonaphthalenesulfonate); EDTA, ethylenediaminetetraacetic acid; EGTA, [ethylenebis(oxyethylenetriamino)]tetraacetic acid; GTP, guanosine 5'-triphosphate; MES, 2-(N-morpholino)ethanesulfonic acid; PIPES, 1,4-piperazinediethanesulfonic acid.

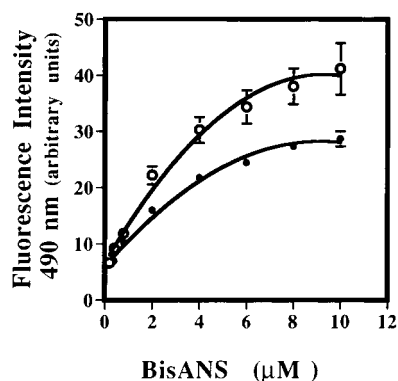


FIGURE 2: Concentration-dependent binding of BisANS to $\alpha\beta_{II}$ and $\alpha\beta_{III}$. Aliquots of $\alpha\beta_{II}$ (○) and $\alpha\beta_{III}$ (●) at 2 μ M were mixed with BisANS to final concentrations ranging from 0.2 to 10 μ M. The fluorescence intensity was measured immediately. Standard deviations are shown.

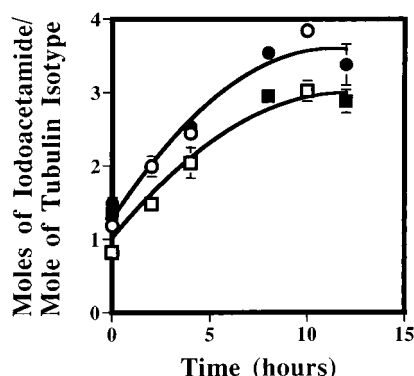


FIGURE 3: Exposure of sulfhydryls on $\alpha\beta_{II}$ and $\alpha\beta_{III}$ during decay. Samples of $\alpha\beta_{II}$ [data sets one (○) and two (●)] and $\alpha\beta_{III}$ [data sets one (□) and two (■)] at 4 μ M were allowed to decay at 37 °C. At the times indicated, iodo[14 C]acetamide (538 μ Ci/mM) was added to a final concentration of 400 μ M. Data shown are from two experiments in which the amount of iodo[14 C]acetamide which reacted with each tubulin isotype was determined. Triplicate samples were taken at 0, 2, 4, and 10 h in the first and quadruplicate samples were taken at 0, 4, 8, and 12 h in the second. Standard deviations are shown.

BisANS, the initial binding of BisANS to $\alpha\beta_{III}$ was 68.5 \pm 0.1% of that binding to $\alpha\beta_{II}$.

Similar results were obtained when the exposure of sulfhydryl groups was measured. The $\alpha\beta_{II}$ and $\alpha\beta_{III}$ dimers were incubated at 37 °C and titrated with iodo[14 C]acetamide at different times (Figure 3). The graph is a composite of data from two separate experiments. There were fewer titratable sulfhydryls on $\alpha\beta_{III}$ than on $\alpha\beta_{II}$, and the rate of appearance of sulfhydryls was also slower for $\alpha\beta_{III}$ than for $\alpha\beta_{II}$. The reaction with iodo[14 C]acetamide reached a plateau at approximately 3.6 mol/mol of $\alpha\beta_{II}$ and 2.9 mol/mol of $\alpha\beta_{III}$.

Colchicine binding is the classic assay for tubulin decay (14); in Figure 4, the rate of loss of the ability to bind colchicine was compared for $\alpha\beta_{II}$ and $\alpha\beta_{III}$. The experiment was done in triplicate and showed that $\alpha\beta_{II}$ lost the ability to bind colchicine with a half-time of 6.3 h, whereas the half-time for loss of colchicine binding to $\alpha\beta_{III}$ was 7.7 h. A repeat of the experiment (data not shown), using quadruplicate samples, indicated half-times for loss of colchicine binding to be 5.9 h for $\alpha\beta_{II}$ and 7.7 h for $\alpha\beta_{III}$.

Differential scanning calorimetry was used to monitor the heat induced protein unfolding transitions of the isotypically

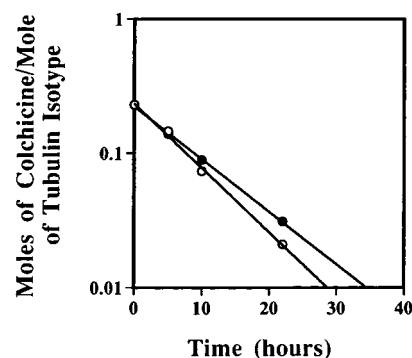


FIGURE 4: Loss of colchicine binding to $\alpha\beta_{II}$ and $\alpha\beta_{III}$ during decay. Samples of $\alpha\beta_{II}$ (○) and $\alpha\beta_{III}$ (●) at 4 μ M were incubated at 37 °C for 22 h. Aliquots were removed, and [3 H]colchicine (100 Ci/M) at a final concentration of 10 μ M was used to measure colchicine binding. Triplicate samples were taken; standard deviations are smaller than the symbols. The half times for loss of colchicine binding were 6.3 h for $\alpha\beta_{II}$ and 7.7 h for $\alpha\beta_{III}$.

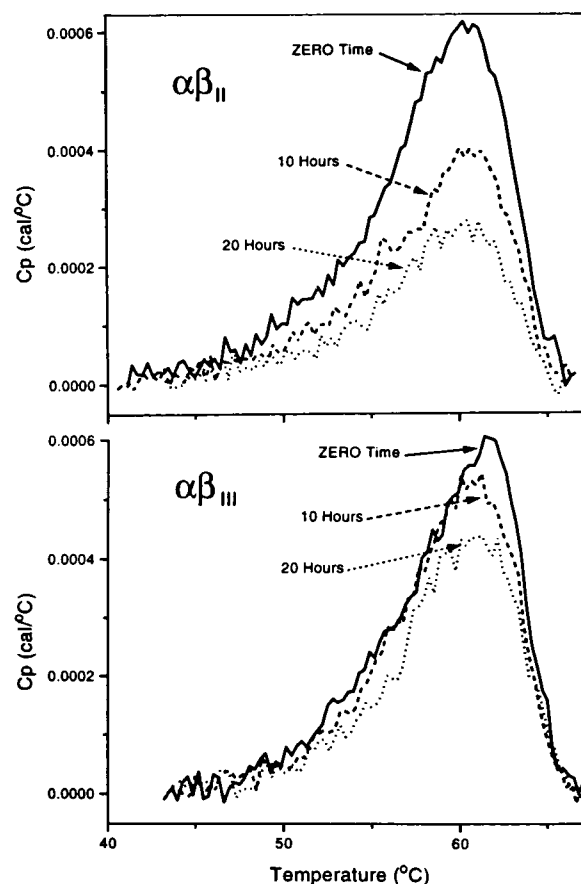


FIGURE 5: Loss of tertiary structure by $\alpha\beta_{II}$ and $\alpha\beta_{III}$ during decay. Samples of $\alpha\beta_{II}$ (2.5 mg/mL) and $\alpha\beta_{III}$ (2.7 mg/mL) were allowed to decay at 0 °C. Aliquots were removed at 0, 10, and 20 h and scanned in a microcalorimeter. These scans were plotted as heat capacity (C_p) versus temperature. Scans of $\alpha\beta_{II}$ are shown in the upper panel, $\alpha\beta_{III}$ in the lower panel.

purified dimers. Samples of $\alpha\beta_{II}$ (2.5 mg/mL) and $\alpha\beta_{III}$ (2.7 mg/mL) were allowed to decay at 0 °C for 20 h. Aliquots were scanned in an MC-2 microcalorimeter at 0, 10, and 20 h. Figure 5 compares two series of unfolding transitions; the top panel for $\alpha\beta_{II}$ and the lower for $\alpha\beta_{III}$. Although the area under the curves decreased with time, the simple character of the endothermic peaks did not change. This decrease was more pronounced in the case of $\alpha\beta_{II}$ than it was for $\alpha\beta_{III}$. Over time, as decay proceeded, there was also

Table 1: Parameters of Unfolding Transitions

isotype	time at 0 °C (h)	enthalpy of unfolding (kcal mol ⁻¹) ^a	T _m (°C) ^b	peak width T _{1/2} (°C) ^b	percent folded ^c
$\alpha\beta_{II}$	0	180 ± 9	60.3 ± 0.1	8.1 ± 0.1	100
	10	128 ± 6	60.1 ± 0.1	8.1 ± 0.1	71 ± 5
	20	86 ± 4	60.5 ± 0.1	7.8 ± 0.1	48 ± 3
$\alpha\beta_{III}$	0	168 ± 8	61.4 ± 0.1	7.2 ± 0.1	100
	10	151 ± 8	61.2 ± 0.1	8.1 ± 0.1	90 ± 6
	20	125 ± 6	61.2 ± 0.1	6.9 ± 0.1	74 ± 5

^a Designation of slopes for the pretransition and post-transition baselines used to extrapolate the baseline heat capacity across the transition region introduced an error of 5% in the calculation of the area under the transition curve which was used to calculate kilocalories per mole. ^b Instrumental error. ^c Percent folded was calculated from the enthalphy of unfolding taking the enthalpy at zero time as 100%.

no apparent shift in the melting temperatures (the midpoints of the unfolding transition). The same experiments done at lower isotype concentrations showed that these observations were not concentration dependent (data not shown). Table 1 contains values for several parameters associated with the unfolding transitions. To analyze a transition curve, the low-temperature baseline, representing the specific heat capacity of the folded molecules, and the high-temperature baseline, representing the specific heat capacity of the unfolded molecules, were extrapolated across the transition region using the progress baseline as calculated by the Origin program supplied by MicroCal, Inc. The area under the curve above the merged baselines represented the enthalpy of unfolding. In Table 1, column 3, the enthalpy of unfolding is expressed as kilocalories absorbed per mole of tubulin isotype. The melting temperatures are shown in column 4. The melting temperature of $\alpha\beta_{III}$ was marginally, but consistently, higher than the melting temperature of $\alpha\beta_{II}$. The peak widths measured at half the peak heights are shown in column 5. They remained stable throughout the course of the experiment for both isotypes and did not show a broadening or narrowing trend. In the last column, considering that the area under the transition curve of a scan is proportional to the amount of protein making the transition from folded to random coil, the enthalpy of unfolding values were used to estimate the percentage of each isotype retaining tertiary structure at the 10 and 20 h time points. Figure 6 compares the decay experiments shown in Figure 5 and identical experiments done at lower isotype concentrations (transition curves not shown). The natural logarithms of the enthalpy of unfolding values for $\alpha\beta_{II}$ and $\alpha\beta_{III}$ were plotted versus time. A decay rate constant and half-life calculated from each data set is shown in Table 2.

DISCUSSION

Studies using chemical probes consistently showed that $\alpha\beta_{III}$ was more resistant to the conformational changes associated with decay than was $\alpha\beta_{II}$. Prasad et al. first reported that decay results in the exposure of hydrophobic areas on the tubulin molecule (16). Because the apolar probe BisANS fluoresces intensely in media of low dielectric constant, it is a sensitive reporter of solvent-accessible hydrophobic regions on the surface of proteins (21). Figure 1 shows that, as anticipated, both $\alpha\beta_{II}$ and $\alpha\beta_{III}$ bound more BisANS as they decayed. The increase in fluorescence

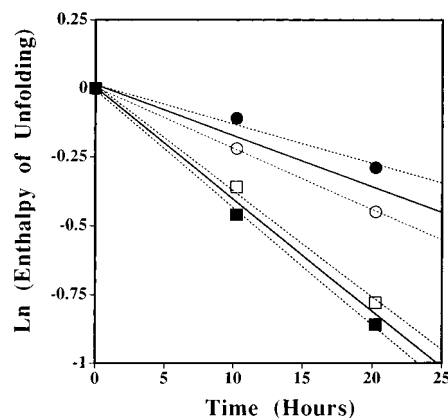


FIGURE 6: Comparison of the decay rates of $\alpha\beta_{II}$ and $\alpha\beta_{III}$. Samples of $\alpha\beta_{II}$ [2.5 mg/mL (■); 1.6 mg/mL (□)] and $\alpha\beta_{III}$ [2.7 mg/mL (●); 1.4 mg/mL (○)] were allowed to decay at 0 °C. At 0, 10, and 20 h, aliquots were removed and scanned in a microcalorimeter. Areas under the transition curves were used to calculate enthalpy of unfolding values. The natural logarithms of the enthalpy of unfolding values were plotted versus time. Values were normalized to the same y-intercept for ease of comparison. Dotted lines are best fit lines for individual data sets; solid lines are best fit lines for the combined $\alpha\beta_{II}$ data and the combined $\alpha\beta_{III}$ data.

Table 2: Rate Constants of Unfolding

isotype	concentration (mg mL ⁻¹)	rate constant k (10 ⁻³ h ⁻¹) ^a	half-life (h) ^b
$\alpha\beta_{II}$	2.51	43 ± 2	17 ± 1
	1.57	39 ± 3	18 ± 1
$\alpha\beta_{III}$	2.70	14 ± 3	50 ± 9
	1.38	22 ± 1	32 ± 1

^a Errors are the standard deviations of the slopes calculated using the Origin computer program. ^b Errors were calculated using the standard deviations of the slopes shown in column three.

intensity occurred more rapidly for $\alpha\beta_{II}$ than for $\alpha\beta_{III}$, indicating that $\alpha\beta_{II}$ more easily undergoes the conformational changes that make additional hydrophobic sites accessible to the probe. Ward and Timasheff reported that BisANS binding to unfractionated tubulin is characterized by one high-affinity site and 40–50 lower affinity sites (22). The lower affinity sites appear to be related in a positively cooperative manner, which is consistent with binding being accompanied by a loosening of the protein structure. The enhanced binding of BisANS to $\alpha\beta_{II}$ (Figure 1) might result from a greater degree of cooperativity among the lower affinity binding sites of this isotype. Data shown in Figure 2 also indicate that $\alpha\beta_{II}$ and $\alpha\beta_{III}$ interact differently with BisANS. At substoichiometric BisANS:isotype ratios, binding of the probe is essentially the same. Since binding at low BisANS concentrations is predominantly to the single high affinity site on the β -subunit (23), it appears that $\alpha\beta_{II}$ and $\alpha\beta_{III}$ are very similar with respect to their high-affinity binding sites. At stoichiometric ratios greater than 1:1, the higher fluorescence intensities of BisANS bound to $\alpha\beta_{II}$ indicate greater surface hydrophobicity. Since at higher BisANS concentrations binding to the low-affinity sites would be more significant, this increased surface hydrophobicity of $\alpha\beta_{II}$ might reflect the presence of more low-affinity binding sites or, as suggested earlier, the same number of sites related by a higher degree of positive cooperativity. Sarkar et al. also studied the phenomenon of enhanced BisANS binding to unfractionated tubulin as it decayed and

reported that the extent of fluorescence enhancement was inversely related to the protein concentration (24). Using the method of Panda et al. (25), they calculated the percentage of monomer and dimer present at the tubulin concentrations studied and showed a positive correlation between the conformational changes associated with enhanced BisANS binding and the fraction of tubulin in monomeric form. Since the possibility exists that the lower affinity BisANS binding sites are located in the dissociated subunits, the different rates at which $\alpha\beta_{II}$ and $\alpha\beta_{III}$ acquire enhanced BisANS fluorescence could be related to differences in dissociation constants of the dimers.

Sulfhydryl groups are sensitive reporters of the effects of ligands on the tubulin molecule (26). It has been shown that BisANS binding at low concentrations has little effect on alkylation while binding at high concentrations strongly enhances alkylation of unfractionated tubulin (27). This suggests that conformational changes resulting from BisANS binding at the positively cooperative low-affinity sites increase the accessibility of sulfhydryls as well as the hydrophobic sites which result in more BisANS binding. Therefore, it is not surprising that the conformational changes which occur during decay enhance not only BisANS binding but also alkylation. Figure 3 shows the increasing accessibility of sulfhydryls to alkylation by iodo[^{14}C]acetamide as $\alpha\beta_{II}$ and $\alpha\beta_{III}$ decay. These studies suggest slightly higher levels of alkylation of $\alpha\beta_{II}$ at zero time which is consistent with studies by Sharma and Ludueña (7) showing that Cys¹² can be cross-linked with either Cys²⁰¹ or Cys²¹¹ in $\alpha\beta_{II}$ but not in $\alpha\beta_{III}$. The higher levels of incorporation of iodo[^{14}C]acetamide into $\alpha\beta_{II}$ indicated that the conformation of $\alpha\beta_{II}$ was perturbed to a greater extent than the conformation of $\alpha\beta_{III}$.

Colchicine-binding experiments (Figure 4) indicated small but reproducible differences in the isotype-specific loss of colchicine binding. The half-time for loss of colchicine binding by $\alpha\beta_{II}$ averaged 6.2 h; whereas the half-time for loss of binding by $\alpha\beta_{III}$ was consistently 7.7 h. Although the colchicine-binding site has been reported to involve both the α - and β -subunits (28, 29), the β -subunit composition clearly influences the stability of the colchicine-binding site. These results are consistent with an earlier study by Banerjee and Ludueña (4), which showed that the association rate constants for the interactions of isotypically purified dimers with colchicine were different, with $\alpha\beta_{II}$ binding colchicine four times faster than does $\alpha\beta_{III}$. Since binding involves conformational changes in both tubulin and colchicine (30, 31), these results suggest that $\alpha\beta_{II}$ is more flexible than $\alpha\beta_{III}$. A subsequent study showed that desacetamidocolchicine, a colchicine analogue lacking the B-ring acetamido group, bound to isotypically purified dimers by a two-step mechanism. The fast initial step forming a low-affinity complex did not differ significantly among the isotypes, but the second slow step involving a conformational change was approximately 10 times slower for $\alpha\beta_{III}$ than for $\alpha\beta_{II}$ or $\alpha\beta_{IV}$, providing more conclusive evidence that $\alpha\beta_{II}$ is more flexible than $\alpha\beta_{III}$ (32). Considered in conjunction with the current studies, it would seem that the flexibility of $\alpha\beta_{II}$ makes it less resistant to decay-related conformational changes, whereas, the less flexible nature of $\alpha\beta_{III}$ contributes to its stability.

Differential scanning calorimetry revealed some unexpected information regarding the heat-induced unfolding of the isotypically purified dimers and the nature of the decay process. First, the initial scans of the isotypes shown in Figure 5 indicated that both isotypes unfolded in a highly cooperative manner. The unfolding transitions appeared to be single endothermic peaks. It was surprising, given the complexity and size of the tubulin molecule, that there were no resolvable multiple transitions. Partially unfolded intermediates were apparently so unstable relative to the fully folded and fully unfolded conformations that they could not be detected. These unfolding transitions were completely irreversible. It is not possible to state at which point the α - and β -subunits separated. The unfolding transitions may reflect monomerization followed by rapid loss of tertiary structure. However, since the energy input required to separate the subunits would be small compared to the energy necessary to disrupt the tertiary structure, dissociation could have occurred undetected at a lower temperature and the transitions would then represent only the unfolding of the monomers. At the elevated temperatures at which the calorimetric unfolding transitions occurred ($\sim 60^\circ\text{C}$), the slightly higher melting temperature (T_m) of $\alpha\beta_{III}$ was the only hint of its increased stability that could be obtained from the zero time scans. On the basis of a comparison of three scans of each isotype at concentrations from 1.4 to 2.7 mg/mL, it was estimated that the melting temperature of $\alpha\beta_{III}$ was $1.2 \pm 0.6^\circ\text{C}$ higher than that of $\alpha\beta_{II}$.

Second, decay also appears to be a cooperative process. Scans of partially decayed isotypes at 10 and 20 h (Figure 5) still contained only one transition peak. The melting temperatures did not shift and the peak widths did not broaden (Table 1). To interpret this observation, it was necessary to determine what changes would occur in the unfolding transition of tubulin when its conformation was intentionally perturbed. Therefore, for diagnostic purposes, calorimetry scans of unfractionated tubulin were done in the presence of urea or ethanol (data not shown). The changes observed in the presence of these denaturants provided information which helped interpret the calorimetric scans shown in Figure 5. The thermal unfolding transition of unfractionated tubulin consisted of a single endothermic peak at 61°C which shifted to 58°C when tubulin was scanned in 0.5 M urea; when tubulin was scanned in 20% ethanol, the unfolding transition appeared to resolve into two peaks at 42 and 49°C , although precipitation of the unfolded tubulin at $\sim 51^\circ\text{C}$ made positive identification of the peak at 49°C questionable (data not shown). We concluded that if the decay process had resulted in the partial unfolding of essentially all molecules present, the single transition peak would have shifted to a lower melting temperature just as it did when tubulin was converted from its native conformation to a molten globule in the presence of urea. If decay resulted in the formation of subpopulations of partially unfolded molecules, this shift might be accompanied by the appearance of other peaks similar to the changes observed in ethanol. However, the only change observed in the scans of the isotypes as they decayed was a decrease in the area under the transition curves. This decrease in enthalpy of unfolding (Table 1) indicated that, with time, increasing numbers of molecules of both isotypes were already fully denatured prior

to the heat-induced unfolding observed in the calorimeter. The position of the unfolding transition of the molecules which still retained tertiary structure (Figure 5, Table 1) indicated that their conformation was the same as it was at the time of the initial scan. Since no partially decayed intermediates were detected, it can be speculated that once an initial conformational change triggers the decay process the molecule rapidly unfolds.

Evidence that 74% of the $\alpha\beta_{III}$ molecules remained folded after 20 h, as compared to only 48% of the $\alpha\beta_{II}$, indicated that $\alpha\beta_{III}$ was more resistant to the disruptive forces that trigger decay. A comparison of the decay experiments shown in Figure 6 estimated $\alpha\beta_{III}$ to be more stable than $\alpha\beta_{II}$ by a factor of 2 (Table 2).

Although in vitro evidence for conformational and stability differences between $\alpha\beta_{III}$ and other $\alpha\beta$ dimers abounds, the in vivo relevance remains elusive. What is the reason for the prevalence of $\alpha\beta_{III}$ in neuronal tissue or the elevation in various tumors when it is not present in the normal tissues? Could the presence of $\alpha\beta_{III}$ impart a greater stability to the cytoskeleton of long-lived cells, such as neurons, or perhaps affect the little understood role of tubulin in cell signaling pathways which initiate protein synthesis and cell division? It is reasonable to speculate that a more stable isotype would be more resistant to proteolytic degradation in vivo. Certainly, conditions in vivo are likely to affect tubulin stability. For example, high concentrations of bovine serum are known to stabilize tubulin in vitro (33). It is not unreasonable that tubulin decay in the cell could be inhibited by the high protein concentrations particularly if some of these proteins are chaperonins. Also, recycling of tubulin molecules into and out of microtubules may prolong their stability. Nevertheless, our finding that $\alpha\beta_{II}$ and $\alpha\beta_{III}$ differ in their relative stabilities in vitro in a variety of conditions suggests that their stabilities may also differ in vivo, even if their decay rates are slower in the cell. Therefore, speaking in general terms, it is possible that differences in stability of tubulin isotypes, together with differences in their expression, may provide cells with a responsive and flexible mechanism for adapting the dynamic and ligand-binding properties of their microtubules so as to best serve the requirements of the cell. A comparison of isotype turnover rates in cultured cells, such as rat PC-12 cells which extend neurites in response to nerve growth factor (34), would be one approach to determine if the greater stability of $\alpha\beta_{III}$ observed in vitro is evident in intact cells and bring us closer to an understanding of the in vivo significance of tubulin isotypes.

ACKNOWLEDGMENT

We thank Dr. Barry Nall for use of the MC-2 microcalorimeter and for reading related sections of this manuscript. We extend our appreciation to Dr. Asok Banerjee, Dr. Asish Chaudhuri, and Dr. Israr Khan for insightful discussions and to Mohua Banerjee, Veena Prasad, and Consuelo Walss for technical assistance in preparation of unfractionated bovine brain tubulin.

REFERENCES

1. Ludueña, R. F. (1993) *Mol. Biol. Cell* 4, 445–457.
2. Banerjee, A., Roach, M. C., Trcka, P., and Ludueña, R. F. (1992) *J. Biol. Chem.* 267, 5625–5630.
3. Panda, D., Miller H. P., Banerjee, A., and Wilson, L. (1994) *Proc. Natl. Acad. Sci. U.S.A.* 91, 11358–11362.
4. Banerjee, A., and Ludueña, R. F. (1992) *J. Biol. Chem.* 267, 13335–13339.
5. Khan, I. A., and Ludueña, R. F. (1995) *Mol. Biol. Cell* 6, 30a.
6. Derry, W. B., Wilson, L., Khan, I. A., Ludueña, R. F., and Jordan, M. A. (1994) *J. Protein Chem.* 13, 165–176.
7. Sharma, J., and Ludueña, R. F. L. (1994) *J. Protein Chem.* 13, 165–176.
8. Lopata, M. A., and Cleveland, D. W. (1987) *J. Cell Biol.* 105, 1707–1720.
9. Joshi, H. C., and Cleveland, D. W. (1989) *J. Biol. Chem.* 109, 663–673.
10. Joshi, H. C., Yen, T. Y., and Cleveland, D. W. (1987) *J. Biol. Chem.* 105, 2179–2190.
11. Hoyle, H. D., and Raff, E. C. (1990) *J. Cell Biol.* 111, 1009–1026.
12. Joshi, H. C., and Cleveland, D. W. (1990) *Cell Motil. Cytoskel.* 16, 159–163.
13. Sisodia, S., Gay, D. A., and Cleveland, D. W. (1990) *N. Biologist* 2, 66–76.
14. Wilson, L. (1970) *Biochemistry* 9, 4999–5007.
15. Ludueña, R. F., and Roach, M. C. (1981) *Biochemistry* 20, 4437–4444.
16. Prasad, A. R. S., Ludueña, R. F., and Horowitz, P. M. (1986) *Biochemistry* 25, 739–742.
17. Fellous, A., Francon, J., Lennon, A. M., and Nunez, J. (1977) *Eur. J. Biochem.* 78, 167–174.
18. Ludueña, R. F., and Roach, M. C. (1981) *Arch. Biochem. Biophys.* 210, 498–504.
19. Borisy, G. G. (1972) *Anal. Biochem.* 50, 373–385.
20. Liggins, J. R., Sherman, F., Mathews, A. J., and Nall, B. T. (1994) *Biochemistry* 33, 9209–9219.
21. Brand, L., and Gohlke, J. R. (1972) *Annu. Rev. Biochem.* 41, 843–868.
22. Ward, L. D., and Timasheff, S. N. (1994) *Biochemistry* 33, 11891–11899.
23. Ward, L. D., Seckler, R., and Timasheff, S. N. (1994) *Biochemistry* 33, 11900–11908.
24. Sarkar, N., Mukhopadhyay, K., Parrack, P. K., and Bhattacharyya, B. (1995) *Biochemistry* 34, 13367–13373.
25. Panda, D., Roy, S., and Bhattacharyya, B. (1992) *Biochemistry* 31, 9709–9716.
26. Ludueña, R. F., and Roach, M. C. (1991) *Pharmacol. Ther.* 49, 133–152.
27. Ludueña, R. F., Roach, M. C., and Horowitz, P. M. (1986) *Biochim. Biophys. Acta* 873, 143–146.
28. Williams, R. F., Mumford, C. L., Williams, G. A., Floyd, L. J., Aivaliotis, M. J., Martinez, R. A., Robinson, A. K., and Barnes, L. D. (1985) *J. Biol. Chem.* 260, 13794–13802.
29. Floyd, L. J., Barnes, L. D., and Williams, R. F. (1989) *Biochemistry* 28, 8515–8525.
30. Garland, D. L. (1978) *Biochemistry* 17, 4266–4272.
31. Detrich, H. W., III, Williams, R. C., Jr., MacDonald, T. L., Wilson, L., and Pruitt, D. (1981) *Biochemistry* 20, 5999–6005.
32. Banerjee, A., D'Hoore, A., and Engelborghs, Y. (1994) *J. Biol. Chem.* 269, 10324–10329.
33. Solomon, F., Monard, D., and Rentsch, M. (1973) *J. Mol. Biol.* 78, 569–573.
34. Greene, L. A., and Tischler, A. S. (1976) *Proc. Natl. Acad. Sci.* 73, 2424–2428.

BI972763D